RESEARCH ARTICLE SUMMARY

NEURODEVELOPMENT

# Mouse and human share conserved transcriptional programs for interneuron development

**Yingchao Shi†, Mengdi Wang†, Da Mi†, Tian Lu, Bosong Wang, Hao Dong , Suijuan Zhong, Youqiao Chen, Le Sun, Xin Zhou, Qiang Ma, Zeyuan Liu, Wei Wang, Junjing Zhang, Qian Wu*, Oscar Marín*, Xiaoqun Wang***

**INTRODUCTION:** The cerebral cortex contains two main classes of neurons that derive from distinct structures in the developing telencephalon. Excitatory neurons originate from progenitor cells in the developing pallium, whereas γ-aminobutyric acid–expressing (GABAergic) interneurons derive from the ganglionic eminences, the transitory structures of the fetal brain that also give rise to the basal ganglia. The general organization and cellular architecture of the telencephalon are conserved among mammals, but its size and complexity vary enormously between rodents and humans. The extent to which differences in early regulatory mechanisms governing the development of the telencephalon shape fundamental differences in this brain structure in rodents and humans remains elusive.

**RATIONALE:** Despite the substantial progress in characterizing the development of excitatory neurons in the human cerebral cortex, our understanding of the generation of interneurons in the human ganglionic eminences is very limited. In this study, we used single-cell RNA sequencing to obtain the transcriptional profiles of 56,412 single cells in the developing human ganglionic eminences from the late first to the early second trimester of human development (gestational weeks 9 to 18) and applied trajectory inference methods to build the developmental trajectories of the main types of neurons generated in the human ganglionic eminences. We also revealed gene regulatory logic that is likely involved in cell fate specification.

**RESULTS:** We identified molecular features that characterize neural progenitor cells in the human ganglionic eminences. We found that the massive growth of the subventricular zone in the human ganglionic eminences during the second trimester is primarily supported by a large expansion of intermediate progenitor cells. We also revealed the molecular mechanisms underlying the regional specification of progenitor cells as well as the genetic programs driving divergent developmental trajectories in the medial, lateral, and caudal ganglionic eminences (MGE, LGE, and CGE, respectively). In particular, we delineated the developmental trajectories of olfactory bulb neurons, striatal and pallidal GABAergic projection neurons, striatal and cortical GABAergic interneurons, and cholinergic neurons. Despite the protracted development of human cortical interneurons, we found that their diversity is specified within the ganglionic eminences, long before these cells reach the developing cortex. Finally, we identified two populations of human interneurons with features that do not seem to be shared with rodents: a prospective subtype of MGE-derived fast-spiking interneuron and a large population of CGE-derived GABAergic interneurons.

**CONCLUSION:** Our findings reveal the molecular hierarchies governing the development of neurons generated in the human ganglionic eminences. Our results indicate that gene regulatory logic controlling their specification, migration, and differentiation is evolutionarily conserved in mouse and human. We anticipate that these data will advance our understanding of the regulatory mechanisms underlying human brain development. Considering the involvement of striatal and cortical GABAergic neurons in neurodevelopmental disorders such as autism and schizophrenia, our data should enable linking genetic variation to specific cell types to unravel the origin of neurodevelopmental disorders. ■

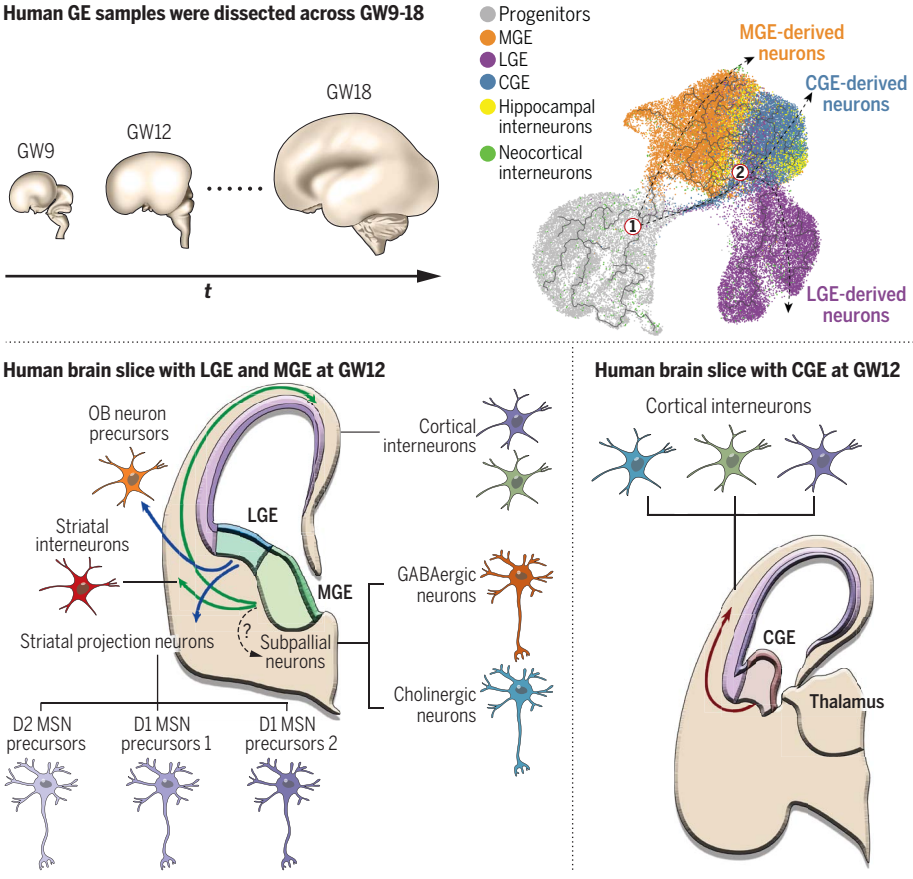


**Developmental trajectories of neurons derived from the human ganglionic eminences.** The main classes of neurons generated from the human medial, lateral, and caudal ganglionic eminences have now been inferred through single-cell transcriptomics. MSN, medium spiny neuron; OB, olfactory bulb; GW, gestational week; *t*, time.

The list of author affiliations is available in the full article online.
*Corresponding author. Email: xiaoqunwang@ibp.ac.cn (X.W.); oscar.marin@kcl.ac.uk (O.M.); qianwu@bnu.edu.cn (Q.W.)
†These authors contributed equally to this work.
Cite this article as Y. Shi *et al.*, *Science* **374**, eabj6641 (2021). DOI: 10.1126/science.abj6641

RESEARCH ARTICLE

NEURODEVELOPMENT

# Mouse and human share conserved transcriptional programs for interneuron development

Yingchao Shi[1]†, Mengdi Wang[1,2]†, Da Mi[3,4,5]†, Tian Lu[1,2], Bosong Wang[6], Hao Dong[1,2], Suijuan Zhong[6,7], Youqiao Chen[6], Le Sun[8], Xin Zhou[1], Qiang Ma[1,2], Zeyuan Liu[1,2], Wei Wang[1,2], Junjing Zhang[6], Qian Wu[6,7]*, Oscar Marín[3,4]*, Xiaoqun Wang[1,2,7,8,9]*

Genetic variation confers susceptibility to neurodevelopmental disorders by affecting the development of specific cell types. Changes in cortical and striatal γ-aminobutyric acid–expressing (GABAergic) neurons are common in autism and schizophrenia. In this study, we used single-cell RNA sequencing to characterize the emergence of cell diversity in the human ganglionic eminences, the transitory structures of the human fetal brain where striatal and cortical GABAergic neurons are generated. We identified regional and temporal diversity among progenitor cells underlying the generation of a variety of projection neurons and interneurons. We found that these cells are specified within the human ganglionic eminences by transcriptional programs similar to those previously identified in rodents. Our findings reveal an evolutionarily conserved regulatory logic controlling the specification, migration, and differentiation of GABAergic neurons in the human telencephalon.

The general organization and cellular architecture of the telencephalon are conserved among mammals, but its size and complexity vary enormously between rodents and primates. Between mouse and human, the cerebral cortex differs 1000-fold in size (*1*, *2*) and varies in the types, proportions, and distributions of cells (*3*–*5*). Global transcriptomic analyses have revealed differences in gene expression patterns between mouse and human (*6*–*10*), whereas single-cell transcriptomic analyses have found conservation in the cellular composition of the cerebral cortex. Most cell types found in rodents, monkeys, and humans are homologous (*11*, *12*). This raises the question of whether the distinctive features of the human telencephalon arise through fundamental changes in the gene regulatory networks controlling the development of this brain structure or through alternative mechanisms.

The cerebral cortex contains two main classes of neurons that derive from distinct structures in the developing telencephalon. Excitatory cortical neurons originate from progenitor cells in the developing pallium, whereas γ-aminobutyric acid–expressing (GABAergic) neurons are generated in the ganglionic eminences, the transitory structures of the fetal brain that also give rise to the basal ganglia (*13*, *14*). Although we have made substantial progress in elucidating the development of excitatory neurons in the human cortex (*14*, *15*), our understanding of the generation of GABAergic neurons in the medial, lateral, and caudal ganglionic eminences (MGE, LGE, and CGE, respectively) is very limited (*16*, *17*). For instance, single-cell transcriptomic studies have identified the molecular signatures of glutamatergic lineages in the developing cortex (*18*–*23*), but similar insights into the development of the human ganglionic eminences remain fragmentary (*10*, *24*). In this study, we investigated the transcriptional trajectories of cells in the developing human ganglionic eminences and found conservation in the genetic programs controlling the development of GABAergic neurons in mice and humans. Our study offers insights into the molecular regulation of neurogenesis and the mechanisms underlying the diversification of GABAergic neurons.

## Cell diversity in the human ganglionic eminences

We used a droplet-based platform to study the transcriptomic profile of individual cells in the developing human ganglionic eminences. To this end, we dissected the ganglionic eminences from gestational weeks (GW) 9 to 18 (table S1), which overlap with the peak of neurogenesis in this region, and performed single-cell RNA sequencing (scRNA-seq). After quality control (fig. S1A), the transcriptional profiles of 56,412 single cells across GW9 to GW18 were obtained and analyzed collectively using unsupervised clustering (Fig. 1A and fig. S1B). Unsupervised clustering of cellular transcriptional identities by uniform manifold approximation and projection (UMAP) dimensionality reduction revealed the existence of 10 cell clusters (Fig. 1B and table S2), which we annotated using well-known cell type–specific markers (Fig. 1C and fig. S1C). The four main clusters correspond to progenitor cells and postmitotic cells from the MGE, LGE, and CGE (Fig. 1B). In addition, we identified smaller cell clusters containing oligodendrocyte progenitor cells (OPCs), microglia, endothelial cells, thalamic neurons, and pallial cells (Fig. 1B). The last two groups derive from tissues adjacent to the ganglionic eminences that were included in the dissection in the smallest samples (Fig. 1A). We used independent samples from two different stages to confirm data repeatability (fig. S1E) and validated the accuracy of unsupervised clustering using a sample in which the MGE, LGE, and CGE were manually dissected and analyzed independently (Fig. 1B). We also performed differential gene expression analysis to detect the genes that best distinguish dividing progenitors from postmitotic cells in the ganglionic eminences, as well as postmitotic cells from the MGE, LGE, and CGE (Fig. 1D, fig. S1D, and tables S3 and S4). Apart from known markers, we identified *NTRK2* (neurotrophic receptor tyrosine kinase 2), which encodes the BDNF (brain-derived neurotrophic factor) and NT-4 (neutrophin-4) receptor (*25*), as a marker of progenitor cells in the human ganglionic eminences (Fig. 1D). Immunohistochemistry staining confirmed that NTRK2 expression is strong in the progenitor domains of the LGE and CGE (Fig. 1E). We also identified genes that distinguish among postmitotic cells with MGE, LGE, and CGE identity, including multiple previously reported regional markers (Fig. 1D, fig. S1D, and table S3), as well as a small population of putative GABAergic neurons among thalamic cells (fig. S1F). Thus, the analysis of cellular transcriptomes revealed regional identities in the developing human ganglionic eminences along with some molecular signatures for specific cell types.

## Conserved genetic regulation of progenitor cells

Neural progenitor cells in the ganglionic eminences (GE progenitors in Fig. 1B) include radial glial cells (RGCs) with neural stem characteristics and intermediate progenitor cells (IPCs), which derive from RGCs and

[1]State Key Laboratory of Brain and Cognitive Science, CAS Center for Excellence in Brain Science and Intelligence Technology (Shanghai), Institute of Biophysics, Chinese Academy of Sciences (CAS), BNU IDG/McGovern Institute for Brain Research, Beijing 100101, China. [2]College of Life Science, University of the Chinese Academy of Sciences, Beijing 100049, China. [3]Centre for Developmental Neurobiology, Institute of Psychiatry, Psychology and Neuroscience, King's College London, London SE1 1UL, UK. [4]MRC Centre for Neurodevelopmental Disorders, King's College London, London SE1 1UL, UK. [5]Tsinghua-Peking Center for Life Sciences, IDG/McGovern Institute for Brain Research, School of Life Sciences, Tsinghua University, Beijing 100084, China. [6]State Key Laboratory of Cognitive Neuroscience and Learning, IDG/McGovern Institute for Brain Research, Beijing Normal University, Beijing 100875, China. [7]Chinese Institute for Brain Research, Beijing 102206, China. [8]Beijing Institute of Brain Disorders, Laboratory of Brain Disorders, Ministry of Science and Technology, Collaborative Innovation Center for Brain Disorders, Capital Medical University, Beijing 100069, China. [9]Guangdong Institute of Intelligence Science and Technology, Guangdong 519031, China.
***Corresponding author. Email: xiaoqunwang@ibp.ac.cn (X.W.); oscar.marin@kcl.ac.uk (O.M.); qianwu@bnu.edu.cn (Q.W.)**
†These authors contributed equally to this work.

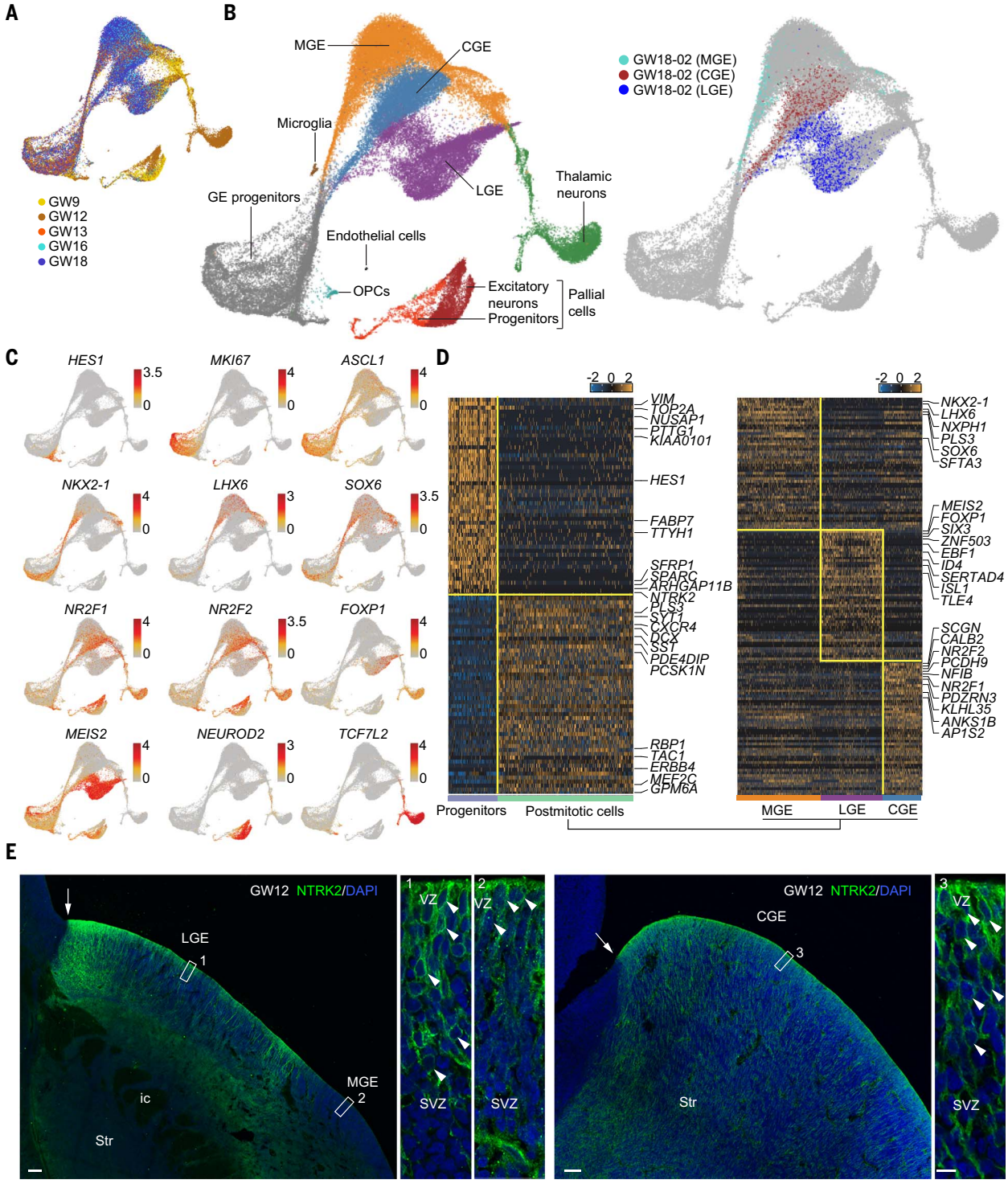


**Fig. 1. Major sources of transcriptional heterogeneity among cells from the human ganglionic eminences.** (**A**) Clustering of individual cells from different gestational weeks visualized by UMAP. (**B**) Annotation of cell clusters on the basis of gene expression. The schema on the right illustrates the distribution of cells obtained from individual dissections of the MGE, LGE, and CGE in relation to the unsupervised clustering of all cells. (**C**) Gene expression visualized by UMAP. Each dot represents an individual cell colored according to the expression level (red, high; gray, low). (**D**) Heatmaps illustrating DEGs enriched in progenitors and postmitotic cells in the ganglionic eminences (left) and among postmitotic cells in the MGE, LGE, and CGE (right). (**E**) Expression of NTRK2 in progenitor cells in the ganglionic eminences at GW12. The areas in white boxes are shown at high magnification. Scale bars, 200 μm (LGE and MGE), 100 μm (CGE), 10 μm (boxes 1 to 3). Str, striatum; ic, internal capsule; DAPI, 4′,6-diamidino-2-phenylindole.

are committed to the neuronal lineage (*16*). We used a list of established markers to delineate both types of progenitor cells in the human ganglionic eminences and visualized their developmental trajectories using pseudotime alignment (Fig. 2A). We then carried out differential gene expression analysis to unbiasedly identify genes whose expression best distinguishes RGCs and IPCs in the human ganglionic eminences (Fig. 2B, fig. S2A, and table S5). In addition to genes that are expressed in progenitor cells in the mouse ganglionic eminences, such as *NES* (nestin), *VIM* (vimentin), *HES1* [hes family basic helix-loop-helix (bHLH) transcription factor 1], and *ASCL1* (achaete-scute family bHLH transcription factor 1), we also found other genes characteristically enriched in progenitor cells. For example, RGCs express *NTRK2* and *FAM107A* (family with sequence similarity 107 member A), while IPCs express *TMSB10* (thymosin beta 10) and *KPNA2* (karyopherin subunit alpha 2) (Fig. 2, A and B).

Progenitor cells in the human ganglionic eminences are spatially organized into two adjacent niches, a relatively thin ventricular zone (VZ) and a large subventricular zone (SVZ) (fig. S2, B to D). In mice, RGCs and IPCs segregate between the VZ and SVZ, respectively. Analysis of gene expression trajectories across pseudo-lamina and pseudo-differentiation axes revealed a similar distribution for RGCs and IPCs in the human ganglionic eminences (Fig. 2C). This organization contrasts with the developing pallium, in which RGCs expressing *FAM107A* and *HOPX* (HOP homeobox) are the most abundant type of progenitor cells in the SVZ (*26*–*28*). We found that most progenitor cells expressing *FAM107A* are in the VZ of the human ganglionic eminences (Fig. 2C and fig. S2C). Although we also detected a small population of RGCs that coexpress *FAM107A* and *HOPX* (Fig. 2A), most progenitor cells in the human ganglionic eminences have the transcriptional signature of IPCs throughout the peak stages of neurogenesis (Fig. 2A).

We used unsupervised clustering to classify progenitor cells in the human ganglionic eminences into 10 transcriptionally distinctive clusters with different gene expression profiles (Fig. 2D and fig. S3A). We observed that these progenitor clusters could be readily segregated according to their regional identity using the expression of genes involved in the patterning of the ganglionic eminences in mice (*29*). For example, expression of *NKX2-1* (NK2 homeobox 1) and *SOX6* (SRY-box transcription factor 6) characterized progenitor cells in the MGE (Fig. 2, D and E; fig. S3B; and table S6). Expression of *PAX6* (paired box 6) was common to progenitor cells in the LGE and CGE, but CGE progenitors were further characterized by the expression of *PROX1* (prospero homeobox 1) and *NR2F2* (nuclear receptor subfamily 2 group F member 2) (Fig. 2, D and E, and figs. S2D and S3B). Further analysis identified *SIX3* (SIX homeobox 3) as a gene differentially expressed among LGE progenitors (Fig. 2E, fig. S3B, and table S6). We validated this later finding using immunohistochemistry and confirmed that SIX3 is highly enriched among dividing progenitor cells in the SVZ of the human LGE from GW10 to GW16 (Fig. 2, F and G). Because *Six3* plays a role in the generation of striatal medium spiny neuron which originate from LGE progenitors in mice (*30*), our results reinforce the notion that eminence-specific genetic programs similar to those described in rodents seem to be involved in the specification of progenitor cells in the human ganglionic eminences.

### Developmental trajectories in the ganglionic eminences

In rodents, the ganglionic eminences give rise to different neuronal populations that populate multiple structures of the adult telencephalon (*30*). The MGE gives rise to GABAergic projection neurons for the globus pallidus, GABAergic interneurons destined for the striatum and cerebral cortex, and cholinergic neurons that remain in the basal telencephalon (*31*–*33*). The LGE primarily produces striatal medium spiny neurons (MSNs) and olfactory bulb (OB) interneurons (*31*, *32*). Finally, the CGE generates GABAergic projection neurons for the amygdala and other limbic system nuclei as well as a diversity of GABAergic interneurons that settle in the cerebral cortex (*34*).

We investigated whether cell diversification among neurons derived from the human ganglionic eminences follows developmental trajectories similar to those described in rodents. We first used a three-dimensional rendering of the distribution of human ganglionic eminence cells in UMAP to identify the relationships between progenitor cells and neurons (fig. S4A and movie S1). We noticed that while most MGE, LGE, and CGE neurons are spatially related to progenitor cells, one group of MGE neurons (which we named MGE-2) was not connected to any group of progenitor cells. This suggested that the progenitor cells of MGE-2 neurons might not have been captured in our dataset, perhaps because they predate the first stage we examined (GW9). We found that MGE-2 neurons express *NKX2-1*, *LHX8* (LIM homeobox 8), *GBX2* (gastrulation brain homeobox 2), and *ISL1* (ISL LIM homeobox 1) (fig. S4B), a combination of genes that are characteristic of subpallial projection neurons, which in the mouse are among the earliest neurons generated in the ganglionic eminences (*35*, *36*). Consistent with this notion, we observed that MGE-2 neurons largely derive from the GW9 and GW12 samples (fig. S4C) and that cells with these features are already present in the human subpallium at GW8 (fig. S4, D and E).

We next integrated our dataset with published scRNA-seq datasets of human neocortical and hippocampal interneurons from GW8 to GW27 (*19*, *20*, *37*), applied trajectory inference methods, and displayed the results via UMAP (Fig. 3, A and B). We excluded MGE-2 neurons from this analysis because their progenitor cells were not likely to be captured in our dataset. We found that most interneurons isolated from the developing neocortex and hippocampus cluster together with MGE and CGE neurons (Fig. 3A and fig. S5A), which is consistent with the view that most cortical interneurons derive from these structures (*17*). Referring to the inferred pseudotime trajectory, we identified the branch points that describe divergences in GE cells on the basis of discrepant gene expression (Fig. 3A and fig. S5B). The results of trajectory inference revealed that the postmitotic cells in the ganglionic eminences first diverge into distinct MGE and LGE or CGE lineages at branch point 1, and that the later lineage subsequently segregates into separate LGE and CGE trajectories at branch point 2 (Fig. 3A).

We then investigated the transcriptional programs driving the divergent developmental trajectories of these cells at each of the branching events. We found pleiotropic genes potentially driving the divergence of cells along each developmental trajectory (Fig. 3C and table S7). For example, *NKX2-1*, *LHX6* (LIM homeobox 6), and *NXPH1* (neurexophilin 1) are enriched in cells that follow the MGE trajectory at branch point 1, whereas *PAX6*, *MEIS2* (Meis homeobox 2), and *NR2F2* are prevalent in cells within the LGE and CGE branch (Fig. 3, D and E, and fig. S5, C and D). We also identified genes enriched in cells that follow LGE [*ZFHX3* (zinc finger homeobox 3), *FOXP1* (forkhead box P1), and *EBF1* (EBF transcription factor 1)] and CGE [*NFIX* (nuclear factor I X), *PROX1*, and *NR2F2*] trajectories at branch point 2, respectively (Fig. 3, D and E, and fig. S5, C and D).

### Transcriptional control of cell specification in the LGE

We next sought to unveil the developmental trajectories of neurons generated in specific regions of the human ganglionic eminences. We first classified human postmitotic LGE cells using unsupervised clustering and performed differential gene expression analysis among the seven resulting clusters (Fig. 4A and fig. S6, A and B). We found that clusters L1 and L2 contain cells expressing *ISL1*, *EBF1*, and *TAC1* (tachykinin precursor 1), which are enriched in striatonigral (D1) MSNs, whereas L4 primarily consisted of cells expressing *PENK* (proenkephalin), a marker of striatopallidal (D2) MSNs. In addition, we observed that genes involved in the development of OB interneurons, such as *CHD7* (chromodomain helicase DNA binding protein 7), *ID2* (inhibitor of DNA

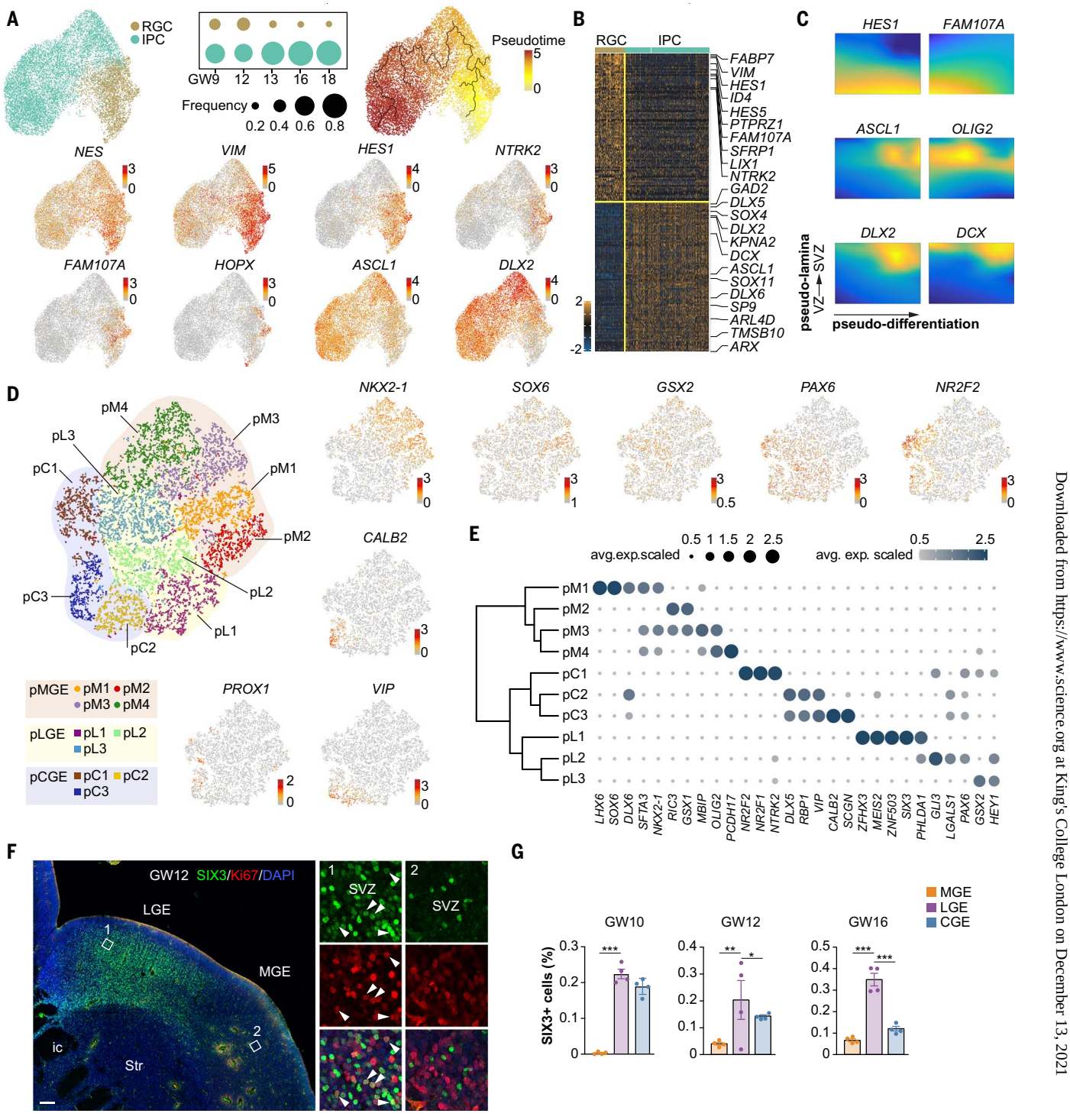


**Fig. 2. Cell diversity and genetic regulation of progenitor cells in the human ganglionic eminences.** (**A**) Clustering of individual progenitor cells in the human ganglionic eminences (top left) and gene expression visualized by UMAP. Each dot represents an individual cell colored according to the expression level (red, high; gray, low). The developmental trajectory of progenitor cells is analyzed via pseudotime alignment (top right). The inset illustrates the ratio of RGCs and IPCs among ganglionic eminence progenitor cells from GW9 to GW18. (**B**) Heatmap illustrating DEGs that distinguish between RGCs and IPCs in the human ganglionic eminences. (**C**) Gene expression patterns along pseudo-differentiation (*x* axis) and pseudo-lamina (*y* axis) coordinates. (**D**) Cell diversity among progenitor cells in the human ganglionic eminences visualized by t-distributed stochastic neighbor embedding (t-SNE). The regional identity of progenitor cells was established according to their characteristic patterns of gene expression. (**E**) DEGs among progenitor cells. The relationships among subclusters of GE progenitors is illustrated via dendrogram. The size of the dots and the color bar were scaled with the average expression of the corresponding genes. (**F**) Expression of SIX3 and Ki67 in the human LGE and MGE at GW12. The areas in white boxes are shown at high magnification. Scale bars, 200 μm (left), 20 μm (right). (**G**) Quantification of the cell ratio of SIX3+ cells in LGE, MGE, and CGE cells at GW10, GW12, and GW16, respectively. Data are presented as means ± SEM ($n$ = 4 samples from three individual experiments; *$P$ < 0.05, **$P$ < 0.01, ***$P$ < 0.001, one-way analysis of variance).

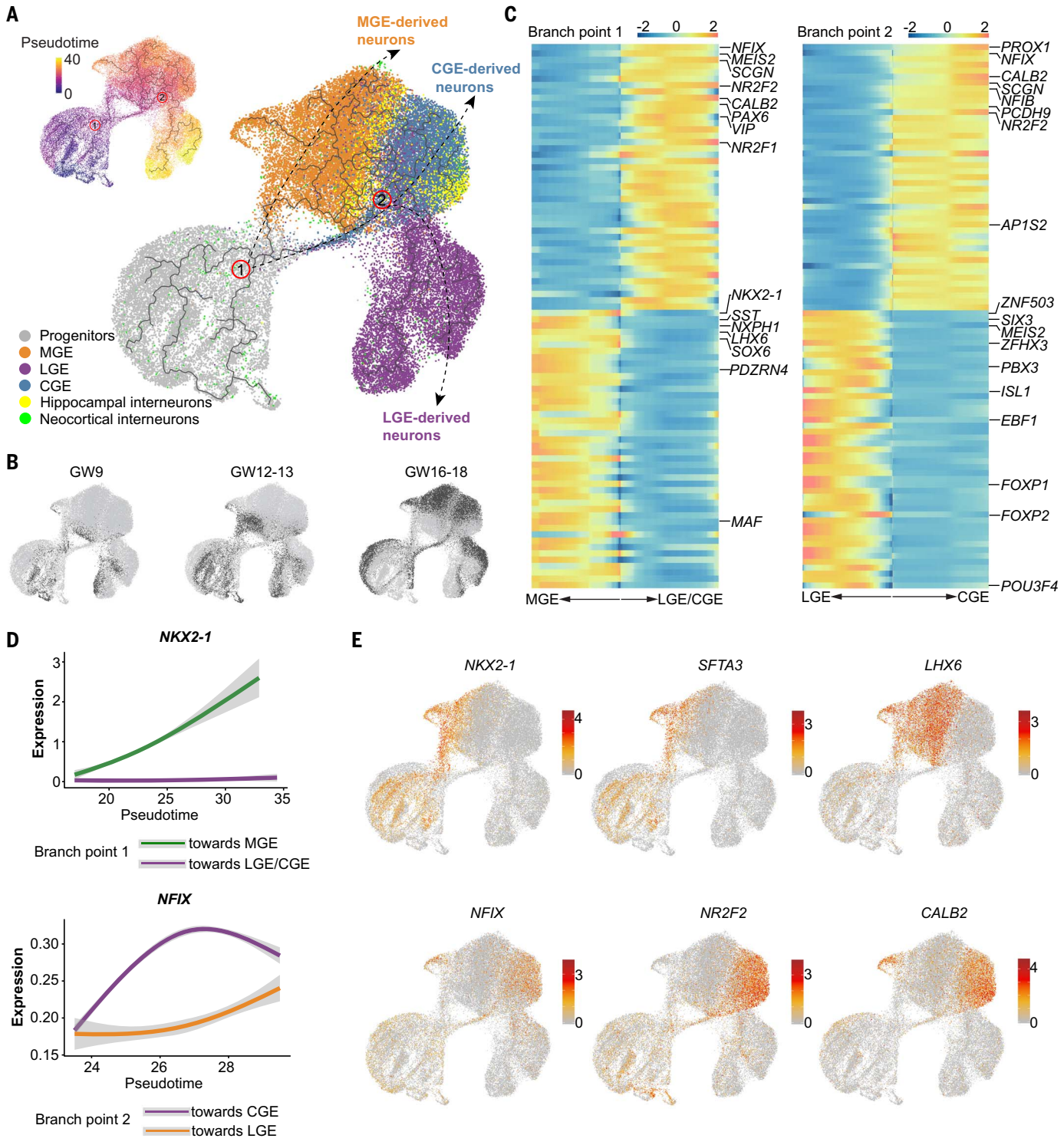


**Fig. 3. Transcriptional programs underlying the developmental divergence of human ganglionic eminences.** (**A**) The cells of human ganglionic eminences and developing cortical and hippocampal interneurons are integrated and visualized by UMAP with inferred trajectories. MGE-2 cells were excluded from this analysis. Potential differentiation trajectories are schematically depicted with arrows. The pseudotime of ganglionic eminence cells is visualized by UMAP (top left). (**B**) Cell distributions at different gestational stages are shown in dark gray. (**C**) Heatmaps illustrating genes linked to cell fate divergence at branch points 1 (left) and 2 (right). (**D**) The expression of *NKX2-1* and *NFIX* diverged at branch point 1 and 2, respectively. (**E**) The expression profile of genes related to cell fate divergence at branch points 1 and 2 is visualized by UMAP. Each dot represents an individual cell colored according to the expression level (red, high; gray, low).

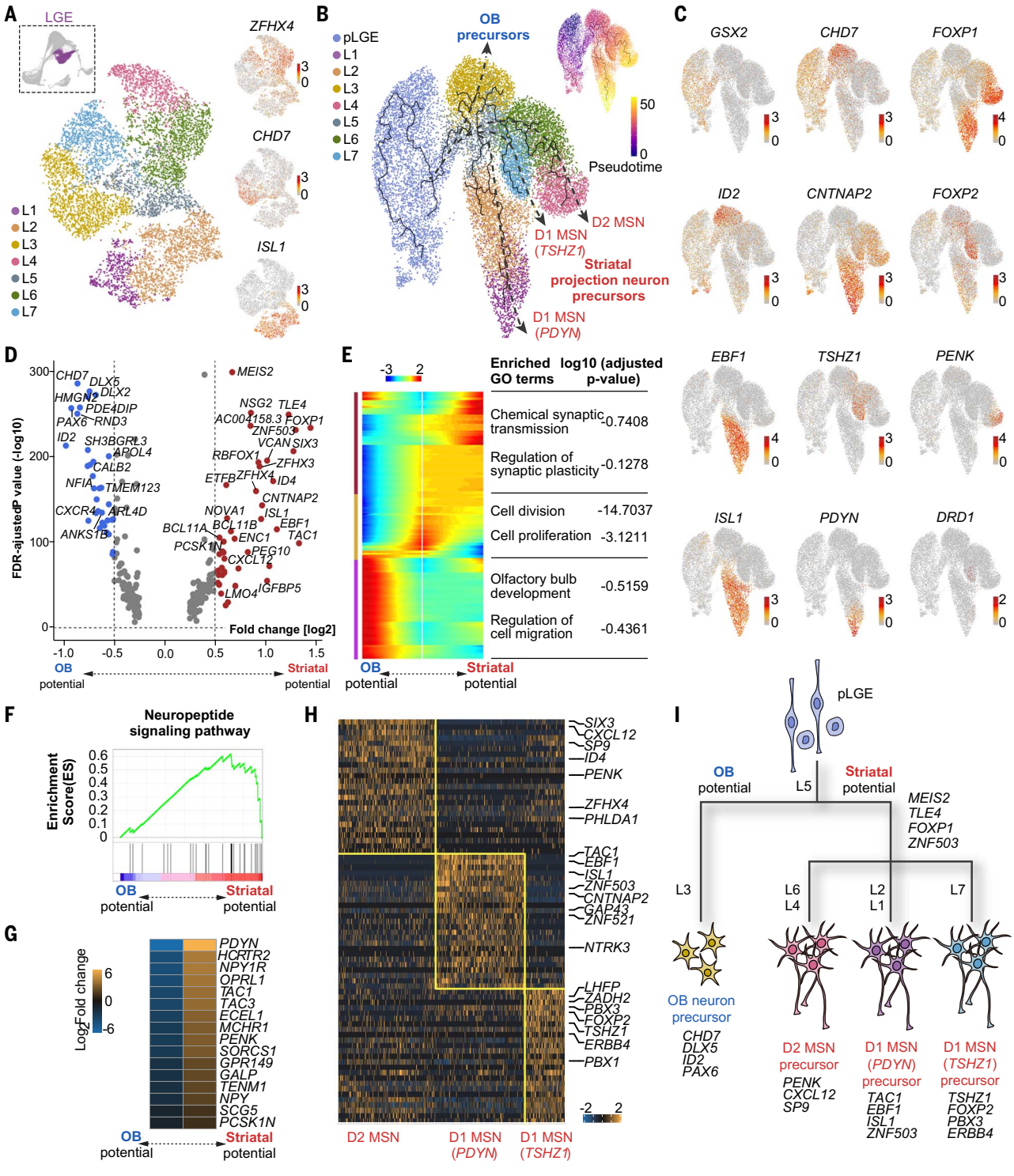


**Fig. 4. Transcriptional regulation of LGE development.** (**A**) Unsupervised clustering of human LGE postmitotic cells and gene expression patterns visualized by t-SNE. Each dot represents an individual cell colored according to the expression level (red, high; gray, low). (**B**) Developmental trajectory of LGE cells visualized by UMAP. Pseudotime for individual cells is also shown (top right). (**C**) Gene expression profile along the developmental trajectories of LGE cells visualized via UMAP. (**D**) Volcano plot of DEGs for LGE cells with OB and striatal potential. (**E**) Heatmap illustrating the bifurcation of gene expression along the developmental trajectory of LGE cells committed to OB and striatal fates. (**F** and **G**) The neuropeptide signaling pathway is enriched in LGE cells with striatal potential. (**H**) Heatmap illustrating DEGs enriched in *TSHZ1*+ D1 MSN, *PDYN*+ D1 MSNs, and D2 MSNs. (**I**) Schematic of hypothetical genetic programs underlying the early diversification of human LGE cells.

binding 2), and *PAX6*, were enriched among L3 cells (Fig. 4A and fig. S6, A and B).

We combined LGE progenitors and postmitotic cells to delineate their developmental trajectories and displayed the results using UMAP (Fig. 4B and fig. S6C). The results of this analysis revealed an early bifurcation of OB and striatal neuron fates, which are delineated by characteristic patterns of gene expression (Fig. 4, B and C). We performed differential gene expression analysis to identify genes potentially driving the divergence of OB and striatal lineages (Fig. 4D and table S8). Gene Ontology (GO) analysis of the differentially expressed genes (DEGs) revealed that GO terms associated with synaptic transmission and plasticity are enriched in LGE cells with striatal potential, whereas GO terms associated with OB development and cell migration are enriched in cells with OB potential (Fig. 4E).

We performed gene set enrichment analysis and found that the neuropeptide signaling pathway was distinctively enriched in the LGE cells with striatum potential (Fig. 4, F and G). We also observed that striatal-specific genes such as *EBF1* and *ISL1* were expressed at earlier stages of development than OB-specific genes such as *CHD7* (fig. S6D), suggesting that LGE cells with striatal potential mature earlier than cells with OB potential. To test this hypothesis, we defined a "maturation score" and mapped the trajectory of LGE postmitotic cells along this inferred trajectory (fig. S6E). This analysis confirmed higher maturation levels for cells with striatum potential than those with OB potential. Further analysis of the developmental trajectories of LGE cells with striatal potential revealed early divergence in three distinct fates, *TSHZ1*+ (teashirt zinc finger homebox 1)+ D1, *PDYN*+ (prodynorphin)+ D1, and D2 MSNs (Fig. 4B), each with a distinctive pattern of gene expression (Fig. 4H). Altogether, our analysis revealed the genetic programs underlying the early diversification of human LGE cells (Fig. 4I).

### Transcriptional control of cell specification in the MGE

To explore neuronal diversity among newborn MGE cells, we classified postmitotic cells from this region using unsupervised clustering (Fig. 5A) and performed differential gene expression analysis among the seven resulting clusters (Fig. 5B and fig. S7, A and B). We found distinctive patterns of gene expression among these cell populations. For example, the largest cluster, M2, contains cells expressing *LHX6* and *SOX6*, two transcription factors that are critical for the development of MGE-derived cortical interneurons (*38*–*41*), and *CXCR4* (C-X-C motif chemokine receptor 4) and *ERBB4* (erb-b2 receptor tyrosine kinase 4), which encode guidance receptors regulating the tangential migration of interneurons from the ganglionic eminences toward the developing cortex (*42*–*46*). In contrast, M5 contains cells expressing *NKX2-1*, *LHX8*, *ISL1*, and *GBX2*, which are characteristic of cholinergic neurons in the subpallium (Fig. 5B) (*33*).

To determine developmental relationships among these clusters, we integrated MGE progenitors and postmitotic neurons with the datasets of developing human cortical and hippocampal interneurons, applied trajectory inference methods (with the exception of MGE-2 cells), and displayed the results using UMAP (Fig. 5C). This analysis revealed that M1 primarily contains undifferentiated precursors that are transitioning toward the acquisition of a distinct cell fate (Fig. 5C). The remaining clusters segregated along two separate trajectories. Branch 1 primarily contained cells from cluster M2 along with most of the developing neocortical and hippocampal interneurons (Fig. 5, C and D). Branch 2 consisted of the small M3 cluster, which contains cells expressing *ETV1* (ETS variant transcription factor 1), *CRABP1* (cellular retinoic acid binding protein 1), and *ANGPT2* (angiopoietin 2) (Fig. 5, C and D, and fig. S7B). This cluster also exhibited high levels of *CXCR4* and *ERBB4* expression (Fig. 5D), suggesting that it may include neurons tangentially migrating to the cortex and consistent with the fact that some more-mature neocortical and hippocampal interneurons also mapped to this branch (Fig. 5C). We also analyzed cell diversity within MGE-2 cells, which comprised a heterogeneous group of cells from the M4, M5, M6, and M7 clusters. We found very few neocortical and hippocampal interneurons among MGE-2 cells (Fig. 5C), which reinforced the idea that cells in these clusters are fated to develop into subpallial neurons. Consistently, we found that these cells segregated into prospective GABAergic (M4 and M7) and cholinergic (M5 and M6) fates with *GAD1* (glutamate decarboxylase 1) and *LHX8* expression, respectively (Fig. 5, D and E), which likely correspond to globus pallidus and cholinergic projection neurons of the basal telencephalon, along with a small number of striatal interneurons. Further analysis of differential gene expression revealed distinctive transcriptional programs that underlie the main developmental trajectories of diversification of human MGE neurons (Fig. 5E).

### Early specification of cortical interneurons

As many 60 different transcriptional identities have been identified among GABAergic neurons in the cerebral cortex of mice and humans (*11*, *12*). To investigate the developmental mechanisms underlying the emergence of interneuron diversity in the adult human neocortex, we focused on the MGE, which gives rise to two main subclasses of cortical GABAergic neurons, parvalbumin-expressing (PV+) and somatostatin-expressing (SST+) cells (*47*). To this end, we integrated cells from the previously identified embryonic M2 and M3 clusters, which likely contain most of MGE-derived tangentially migrating interneuron precursors, with *LHX6*+ cells from two published single-nucleus RNA-seq datasets of the adult human cortex (*11*, *12*) (fig. S8A), and visualized the combined dataset using UMAP (Fig. 5F and fig. S8B). Gene expression profiles indicated that adult *LHX6*+ neurons were allocated to three main subclasses—LHX6+ LAMP5 (lysosomal associated membrane protein family member 5)+, PV+, and SST+ cells (fig. S8B)—which could be further subdivided into multiple types, including PV+ basket cells, PV+ chandelier cells, SST+ Martinotti cells, SST+ non-Martinotti cells, and SST+ long-range projection neurons (Fig. 5F). We then used this classification of adult neurons to annotate M2 and M3 MGE cells on the basis of their transcriptional similarity and found that most of these cells could be assigned to one of the six types identified in the adult cortex (Fig. 5F). Differential gene expression analysis among the embryonic neurons fated to become distinct subclasses of PV+ and SST+ neurons led to the identification of early developmental markers for these populations, many of which continued to be expressed in the corresponding adult interneurons (fig. S8C). This analysis suggested that interneuron diversification, at least at the level of the main interneuron types, is evident in the human MGE long before these cells reach the developing cortex.

We next searched for evidence of fate specification at the level of individual subtypes among human MGE cells. To this end, we focused on SST+ neurons, as they are perhaps the best characterized among the different transcriptional identities observed in the adult cortex (*11*, *12*). We used unsupervised clustering to classify adult SST+ neurons into 13 distinct transcriptional identities: one subtype of long-range projection neuron, six subtypes of Martinotti cells, and six subtypes of non-Martinotti cells (fig. S9, A to F). We then integrated the adult and embryonic datasets and assigned prospective identities to embryonic SST+ cells on the basis of their transcriptional similarity with adult SST+ interneurons (fig. S9G). Using this approach, we identified 11 distinct transcriptional identities ($MGE_{SST}$ 1 to 11) among the embryonic SST+ interneurons that exhibit different patterns of gene expression (fig. S9, G and H). We also conducted an independent, pairwise comparison analysis to define homologies among the embryonic and adult SST+ identities. This analysis revealed that 7 of the 11 embryonic SST+ transcriptional identities identified in the MGE ($MGE_{SST}$ 1, 2, 3, 5, 6, 7, and 10) matched one-to-one with adult SST+ transcriptional subtypes, including one subtype of long-range projection neuron, four Martinotti subtypes, and two non-Martinotti subtypes (Fig. 5G). Our analysis also revealed that four of

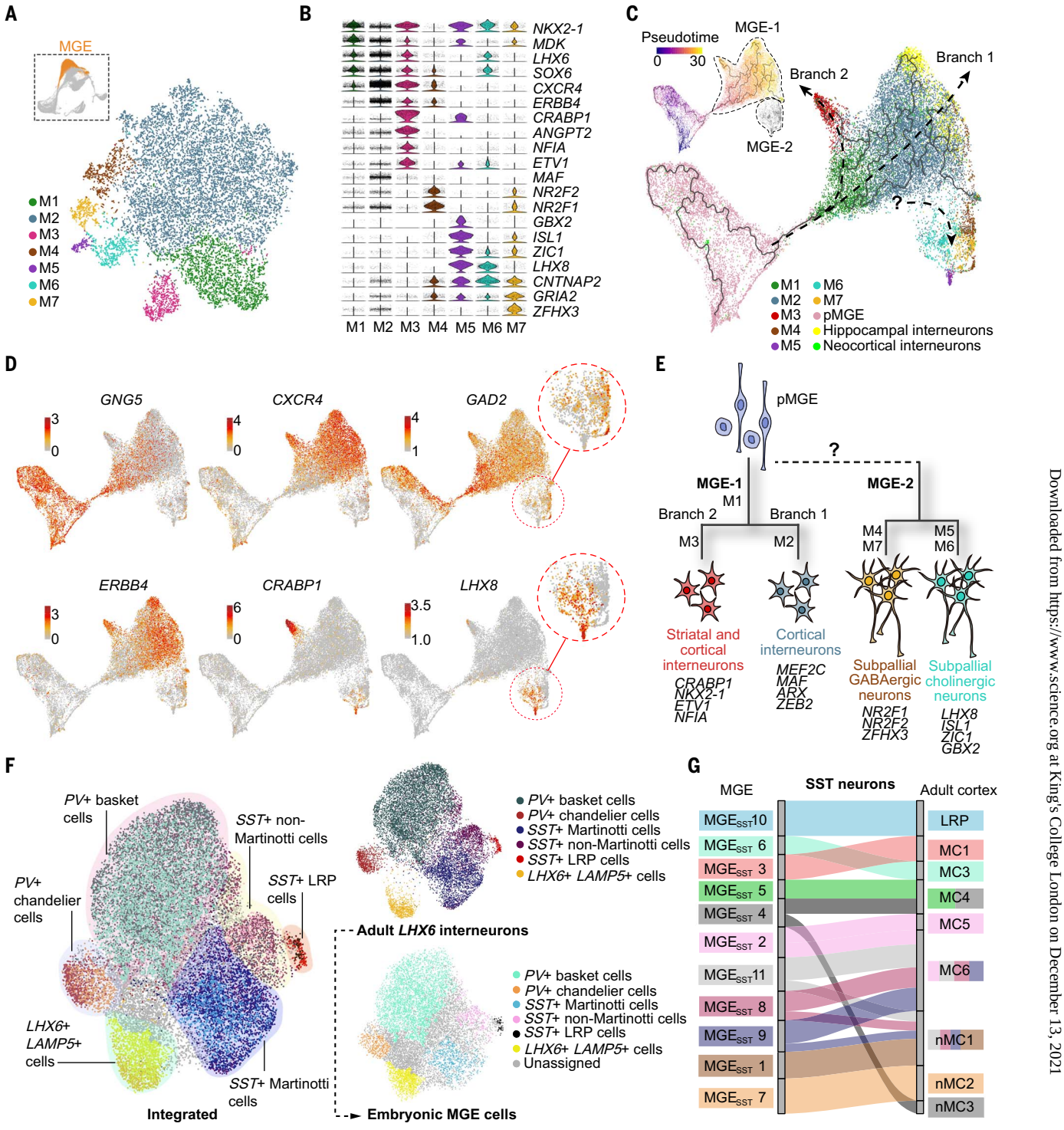


**Fig. 5. Transcriptional control of early cell specification in the human MGE.** (**A**) Neuronal diversity of postmitotic cells in human MGE visualized via t-SNE. (**B**) Violin plots of DEGs among MGE clusters. (**C**) Developmental trajectory of MGE cells are inferred via monocle analysis (with the exception of MGE-2 cells) and visualized by UMAP. Pseudotime of MGE cells in branches 1 and 2 is shown (top left). (**D**) Gene expression along the developmental trajectories of MGE cells is visualized via UMAP. MGE-2 cells comprise GABAergic and cholinergic subpallial neurons, according to the expression of *GAD2* and *LHX8*, respectively. Each dot represents an individual cell and colored according to the expression level (red, high; gray, low). (**E**) Schematic of hypothetical genetic programs underlying the early diversification of human MGE cells. The developmental trajectory linking pMGE (progentiors of the MGE) to MGE-2 cells is uncertain (dotted line) owing to the lack of related progenitor cells in our dataset. (**F**) Integration of postmitotic human MGE cells (M2 and M3) and *LHX6*+ adult human cortical interneurons is visualized by UMAP. MGE cells were annotated according to the classification of adult cortical interneurons on the basis of transcriptional similarities. (**G**) Riverplot illustrating the relationship between MGE cell clusters and adult SST+ interneurons. The size of the bars of MGE cells is normalized to cell numbers. LRP, long-range projection neurons; MC, Martinotti cells; nMC, non-Martinotti cells.

the embryonic SST+ transcriptional identities ($MGE_{SST}$ 4, 8, 9, and 11) share similarities with both the Martinotti cell and non-Martinotti cell lineages (Fig. 5G), perhaps reflecting a relatively immature state. Furthermore, we could not identify embryonic correlates of four adult SST+ transcriptional identities, which are primarily defined by the expression of ion channel genes barely detectable in embryonic interneurons (fig. S9, E and F). Altogether, these results suggest that individual interneuron cell types—as defined by their transcriptional identity—are specified shortly after birth in the human embryonic MGE.

### Distinctive features in developing human interneurons

Despite sharing many cellular features with other species, human cortical interneurons also exhibit some distinctive traits, including morphological and gene expression specializations (*11*, *12*). To investigate whether any of these distinctive characteristics are already embedded in the ganglionic eminences during embryonic development, we integrated our scRNA-seq dataset of human ganglionic eminence cells (GW9 to GW18) with two published datasets of mouse ganglionic eminence cells from embryonic days 12.5 to 14.5 (*48*, *49*) (fig. S10, A and B) and identified 19 cell groups using unsupervised clustering (Fig. 6A, fig. S10C, and table S9). We then calculated the normalized cell ratio of human and mouse cells for each cluster and detected two clusters, 1 and 19, that primarily consisted of human CGE and MGE cells, respectively (Fig. 6B and fig. S10D). We analyzed gene expression in these two predominantly human cell groups and found that cells in each of these clusters exhibit specific markers, such as *SCGN* (secretagogin, EF-hand calcium binding protein), *CALB2* (calbindin 2) and *NR2F2* in cluster 1, and *CRABP1*, *ETV1*, and *NKX2-1* in cluster 19 (Fig. 6C).

We classified human postmitotic CGE cells into three main groups (C1 to C3) using unsupervised clustering (fig. S10E). Cell constitution analysis revealed that most CGE cells at these stages belong to C1 and C2, which exhibit the highest levels of *SCGN* and *CALB2* expression and correspond to cluster 1 (fig. S10F). Immunohistochemical analyses confirmed that cells expressing secretagogin and calretinin, the proteins encoded by *SCGN* and *CALB2*, respectively, concentrate in the SVZ of the human CGE, where they often colocalize with NR2F2 (Fig. 6D and fig. S11A). In contrast, we detected very few SCGN+ cells in the mouse CGE (fig. S11B). In the adult human cortex, secretagogin-expressing neurons are GABAergic and often contain calretinin (Fig. 6E and fig. S11C).

We performed cell constitution analysis for cluster 19 and found that it mainly consisted of M3 cells, characterized by the expression of *CRABP1* and *NKX2-1* (fig. S10G). At GW16, cells coexpressing CRABP1 and NKX2-1, with the typical morphology of migrating interneurons (*46*, *50*), were found in the striatum and en route to the pallium (Fig. 6F). In addition, CRABP1/NKX2-1+ cells were also found in the developing human neocortex (Fig. 6F and fig. S12A). Crabp1/Nkx2-1+ cells could be detected in the mouse subpallium but not in the developing or adult cortex (fig. S12, B and C). In contrast, CRABP1+ cells coexpressing PV were detected in the adult human cortex (Fig. 6G), which suggests that they may represent a population of fast-spiking interneurons.

### Discussion

In this study, we investigated the transcriptional identity of cells in the developing human ganglionic eminences as well as the gene regulatory networks controlling their fate specification. Using single-cell transcriptomics and trajectory inference methods, we built spatiotemporal maps of gene expression through the early second trimester of human development (GW9 to GW18) that recapitulate the developmental trajectories of the main classes of neurons generated in the subpallium, including OB neurons, striatal and pallidal GABAergic projection neurons, cholinergic projection neurons and interneurons, and striatal and cortical GABAergic interneurons. Our results revealed conserved mechanisms underlying the early diversification of subpallial neurons in mouse and human. Although the specific expression of some key factors in the developing human brain, such as *NKX2-1*, *SIX3*, *SCGN*, *CALB2*, *CRABP1*, *ISL1*, and *LHX8*, has been validated via immunostaining, further experiments should investigate their precise involvement in this process.

Newborn neurons are generated from RGCs and IPCs in both ganglionic eminences and developing cortex. The larger primate neocortex is due to a greater number of RGCs, especially basal RGCs in the SVZ, which in rodents is mostly populated by IPCs (*14*, *51*, *52*). Although it has been suggested that a shift toward more basal RGCs may also drive the greater neurogenesis in human than in mouse ganglionic eminences (*16*), we found that the massive growth of the human ganglionic eminence SVZ during the second trimester is primarily due to greater numbers of IPCs. Thus, for the human, the main progenitor cell populations driving neurogenesis in the ganglionic eminences are different from that in the developing cortex.

Previous work has shown that the expression patterns of several transcription factors in the primate ganglionic eminences are very similar to those found in rodents (*17*, *29*). Our transcriptomic analysis reveals that these conserved features extend beyond a handful of key factors and include the complex gene regulatory networks controlling neuronal specification in the human ganglionic eminences. Cortical interneurons in the human ganglionic eminences express the same receptors that have been shown to regulate the tangential migration of interneurons in rodents (*53*). This reveals that the conserved features of human and mouse interneuron development extend beyond the early specification of progenitor cells and involve essential aspects of their subsequent migration and differentiation. Although the roles of some key transcription factors in orchestrating interneuron development have been studied in the mouse, their function in human interneuron development requires experimental validation.

Cortical interneurons are a heterogeneous group of neurons with diverse morphologies, connectivity, biochemistry, and physiological properties (*54*, *55*). In mice, newborn interneurons are transcriptionally heterogeneous within a few hours of becoming postmitotic, and these early transcriptional signatures correlate with those found in specific types of interneurons in the adult cortex (*49*). Our study reveals that interneuron diversification also begins in the human ganglionic eminences, long before these cells reach the developing cortex. For instance, many of the transcriptional identities found among SST+ interneurons in the adult human cortex are identifiable in the MGE. In some cases, however, the transcriptional signature of developing interneurons does not allow a clear correlation with specific adult identities. This is the case for newborn CGE interneurons, most of which are jointly characterized by the expression of *CALB2* and *SCGN*, much like developing CGE interneurons in rodents are characterized by the expression of *Htr3a* (5-hydroxytryptamine receptor 3A) (*56*). *SCGN* encodes a calcium-binding protein similar in sequence and structure to calbindin and calretinin that seems particularly abundant in the developing human brain (*57*, *58*). In the adult human cortex, *SCGN* expression seems to be confined to a small population of GABAergic interneurons whose function remains to be established. We also identified a cluster of human MGE-derived interneurons characterized by the expression of *CRABP1*, which does not seem to have a clear counterpart in rodents. In the mouse, *Crabp1* is expressed by some fast-spiking interneurons in the developing striatum (*59*). In the human, we found that migrating CRABP1-expressing interneurons end up in the adult human cortex and coexpress NKX2-1 and PV. This observation suggests that CRABP1+ cells may represent a population of MGE-derived fast-spiking interneurons in the human cortex.

Although the general cellular architecture of inhibitory cell types is largely conserved, extensive differences seem to exist in the relative proportions, laminar distributions, and gene expression patterns of specific types of

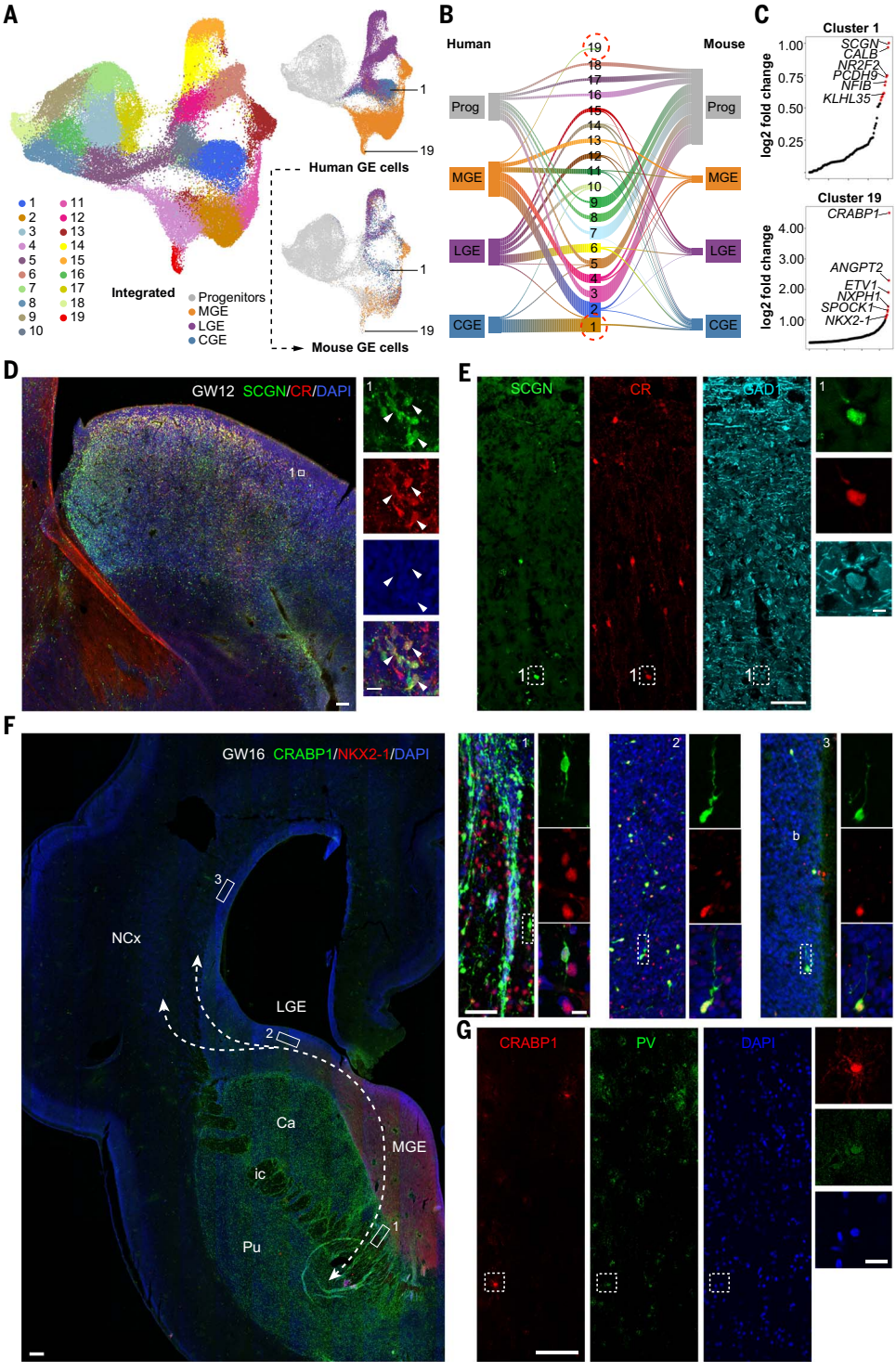


**Fig. 6. Distinctive features of human ganglionic eminences.** (**A**) The datasets of human and mouse ganglionic eminence cells are integrated on the basis of shared sources of variation and visualized by UMAP. (**B**) Riverplot illustrating relationships between human and mouse ganglionic eminence cell clusters. Two human-specific clusters (1 and 19) are highlighted by circles. (**C**) Specific gene expression in human-specific clusters 1 and 19. (**D**) Expression of SCGN and CR in the human CGE at GW12. The area in the white box is shown at high magnification. Scale bars, 100 μm (left) and 20 μm (right). (**E**) Expression of SCGN, CR, and GAD1 in the adult human cortex. The area in the white box is shown at high magnification. Scale bars, 100 μm (left) and 10 μm (right). (**F**) Expression of CRABP1 and NKX2-1 in the embryonic human brain at GW16. The regions in the white boxes are shown at high magnification. The dotted lines illustrate potential migratory routes for CRABP1+ and NKX2-1+ cells. Scale bars, 500 μm (left), 50 μm (boxes 1 to 3, right), 10 μm (boxes 1 to 3, left). NCx, neocortex; Pu, putamen; Ca, caudate. (**G**) Expression of CRABP1 and PVALB in the adult human cortex. The area in the white box is shown at high magnification.

interneurons in the adult cortex of mice and humans. For instance, *LHX6*+ *LAMP5*+ interneurons are much more abundant in the human than in the mouse adult cortex (*11*, *12*). Our findings reveal that human *LHX6*+ *LAMP5*+ interneurons originate in the MGE like their mouse counterparts and shared a common developmental trajectory, which suggests that the differences observed between mouse and human may arise through changes in the dynamics of neurogenesis (*16*) or in the interaction of developing interneurons with the local microenvironment, for instance by means of programmed cell death (*60*).

Neurodevelopmental disorders have overlapping phenotypes and genetics, suggestive of common deficits. Changes in striatal and cortical GABAergic neurons have been extensively documented in autism and schizophrenia (*61*), yet it is presently unclear whether genetic variation associated with these disorders converges on specific types of inhibitory cells because we lack a detailed understanding of their transcriptional trajectories in the developing human brain. Our study sheds light on the development of human GABAergic neurons and should enable the linking of gene

variation and cell types in neurodevelopmental disorders.

### Materials and methods summary

Detailed materials and methods are provided in the supplementary materials. In brief, human fetal ganglionic eminence (GE) samples across gestational weeks (GW) 9 to 18 were collected from Beijing Anzhen Hospital with approval from the Reproductive Study Ethics Committee of Beijing Anzhen Hospital and the institutional review board (ethics committee) of the Institute of Biophysics. Single-cell RNA-sequencing was performed with an Illumina sequencing platform. The outcome reads were aligned to the human reference genome hg19 with Cell Ranger (10X genomics). Doublets were removed by performing the Scrublet pipeline on the raw gene-by-cell expression matrix from each sample (*62*). Batch correction was conducted on the reduced dimensions with the R function of fastMNN (*63*). Seurat was adopted to perform normalization, dimension reduction, unsupervised clustering, and differentially expressed genes identification (*64*, *65*). The Seurat integration method was used to determine the developmental divergence of human GE cells, the early specification of cortical interneurons in human GE, as well as distinctive features of developing human interneurons. The developmental trajectory of human GE cells was constructed using the R package of monocle 3 (*66*–*68*). K-nearest neighbors analysis (knn) was used to render the putative interneuron identities to MGE cells. Immunofluorescence staining was performed on human and mouse brain slices and images were acquired with an Olympus confocal microscope.

### REFERENCES AND NOTES


1. S. Herculano-Houzel, The remarkable, yet not extraordinary, human brain as a scaled-up primate brain and its associated cost. *Proc. Natl. Acad. Sci. U.S.A.* **109** (suppl 1.), 10661–10668 (2012). doi: 10.1073/pnas.1201895109; pmid: 22723358
2. J. DeFelipe, The evolution of the brain, the human nature of cortical circuits, and intellectual creativity. *Front. Neuroanat.* **5**, 29 (2011). doi: 10.3389/fnana.2011.00029; pmid: 21647212
3. J. DeFelipe, L. Alonso-Nanclares, J. I. Arellano, Microstructure of the neocortex: Comparative aspects. *J. Neurocytol.* **31**, 299–316 (2002). doi: 10.1023/A:1024130211265; pmid: 12815249
4. E. Boldog *et al*., Transcriptomic and morphophysiological evidence for a specialized human cortical GABAergic cell type. *Nat. Neurosci.* **21**, 1185–1195 (2018). doi: 10.1038/s41593-018-0205-2; pmid: 30150662
5. N. A. Oberheim *et al*., Uniquely hominid features of adult human astrocytes. *J. Neurosci.* **29**, 3276–3287 (2009). doi: 10.1523/JNEUROSCI.4707-08.2009; pmid: 19279265
6. H. Zeng *et al*., Large-scale cellular-resolution gene profiling in human neocortex reveals species-specific molecular signatures. *Cell* **149**, 483–496 (2012). doi: 10.1016/j.cell.2012.02.052; pmid: 22500809
7. T. E. Bakken *et al*., A comprehensive transcriptional map of primate brain development. *Nature* **535**, 367–375 (2016). doi: 10.1038/nature18637; pmid: 27409810
8. M. Hawrylycz *et al*., Canonical genetic signatures of the adult human brain. *Nat. Neurosci.* **18**, 1832–1844 (2015). doi: 10.1038/nn.4171; pmid: 26571460
9. Y. Zhu *et al*., Spatiotemporal transcriptomic divergence across human and macaque brain development. *Science* **362**, eaat8077 (2018). doi: 10.1126/science.aat8077; pmid: 30545855
10. A. M. M. Sousa *et al*., Molecular and cellular reorganization of neural circuits in the human lineage. *Science* **358**, 1027–1032 (2017). doi: 10.1126/science.aan3456; pmid: 29170230
11. R. D. Hodge *et al*., Conserved cell types with divergent features in human versus mouse cortex. *Nature* **573**, 61–68 (2019). doi: 10.1038/s41586-019-1506-7; pmid: 31435019
12. F. M. Krienen *et al*., Innovations present in the primate interneuron repertoire. *Nature* **586**, 262–269 (2020). doi: 10.1038/s41586-020-2781-z; pmid: 32999462
13. O. Marín, J. L. Rubenstein, A long, remarkable journey: Tangential migration in the telencephalon. *Nat. Rev. Neurosci.* **2**, 780–790 (2001). doi: 10.1038/35097509; pmid: 11715055
14. J. H. Lui, D. V. Hansen, A. R. Kriegstein, Development and evolution of the human neocortex. *Cell* **146**, 18–36 (2011). doi: 10.1016/j.cell.2011.06.030; pmid: 21729779
15. T. Namba, J. Nardelli, P. Gressens, W. B. Huttner, Metabolic regulation of neocortical expansion in development and evolution. *Neuron* **109**, 408–419 (2021). doi: 10.1016/j.neuron.2020.11.014; pmid: 33306962
16. D. V. Hansen *et al*., Non-epithelial stem cells and cortical interneuron production in the human ganglionic eminences. *Nat. Neurosci.* **16**, 1576–1587 (2013). doi: 10.1038/nn.3541; pmid: 24097039
17. T. Ma *et al*., Subcortical origins of human and monkey neocortical interneurons. *Nat. Neurosci.* **16**, 1588–1597 (2013). doi: 10.1038/nn.3536; pmid: 24097041
18. T. J. Nowakowski *et al*., Spatiotemporal gene expression trajectories reveal developmental hierarchies of the human cortex. *Science* **358**, 1318–1323 (2017). doi: 10.1126/science.aap8809; pmid: 29217575
19. X. Fan *et al*., Single-cell transcriptome analysis reveals cell lineage specification in temporal-spatial patterns in human cortical development. *Sci. Adv.* **6**, eaaz2978 (2020). doi: 10.1126/sciadv.aaz2978; pmid: 32923614
20. S. Zhong *et al*., Decoding the development of the human hippocampus. *Nature* **577**, 531–536 (2020). doi: 10.1038/s41586-019-1917-5; pmid: 31942070
21. S. Zhong *et al*., A single-cell RNA-seq survey of the developmental landscape of the human prefrontal cortex. *Nature* **555**, 524–528 (2018). doi: 10.1038/nature25980; pmid: 29539641
22. S. Mayer *et al*., Multimodal Single-Cell Analysis Reveals Physiological Maturation in the Developing Human Neocortex. *Neuron* **102**, 143–158.e7 (2019). doi: 10.1016/j.neuron.2019.01.027; pmid: 30770253
23. Z. Li *et al*., Transcriptional priming as a conserved mechanism of lineage diversification in the developing mouse and human neocortex. *Sci. Adv.* **6**, eabd2068 (2020). doi: 10.1126/sciadv.abd2068; pmid: 33158872
24. V. D. Bocchi *et al*., The coding and long noncoding single-cell atlas of the developing human fetal striatum. *Science* **372**, eabf5759 (2021). doi: 10.1126/science.abf5759; pmid: 33958447
25. M. Bothwell, Functional interactions of neurotrophins and neurotrophin receptors. *Annu. Rev. Neurosci.* **18**, 223–253 (1995). doi: 10.1146/annurev.ne.18.030195.001255; pmid: 7605062
26. S. A. Fietz *et al*., OSVZ progenitors of human and ferret neocortex are epithelial-like and expand by integrin signaling. *Nat. Neurosci.* **13**, 690–699 (2010). doi: 10.1038/nn.2553; pmid: 20436478
27. D. V. Hansen, J. H. Lui, P. R. Parker, A. R. Kriegstein, Neurogenic radial glia in the outer subventricular zone of human neocortex. *Nature* **464**, 554–561 (2010). doi: 10.1038/nature08845; pmid: 20154730
28. A. A. Pollen *et al*., Molecular identity of human outer radial glia during cortical development. *Cell* **163**, 55–67 (2015). doi: 10.1016/j.cell.2015.09.004; pmid: 26406371
29. N. Flames *et al*., Delineation of multiple subpallial progenitor domains by the combinatorial expression of transcriptional codes. *J. Neurosci.* **27**, 9682–9695 (2007). doi: 10.1523/JNEUROSCI.2750-07.2007; pmid: 17804629
30. Z. Xu *et al*., SP8 and SP9 coordinately promote D2-type medium spiny neuron production by activating *Six3* expression. *Development* **145**, dev165456 (2018). doi: 10.1242/dev.165456; pmid: 29967281
31. L. Sussel, O. Marin, S. Kimura, J. L. Rubenstein, Loss of Nkx2.1 homeobox gene function results in a ventral to dorsal molecular respecification within the basal telencephalon: Evidence for a transformation of the pallidum into the striatum. *Development* **126**, 3359–3370 (1999). doi: 10.1242/dev.126.15.3359; pmid: 10393115
32. H. Wichterle, J. M. Garcia-Verdugo, D. G. Herrera, A. Alvarez-Buylla, Young neurons from medial ganglionic eminence disperse in adult and embryonic brain. *Nat. Neurosci.* **2**, 461–466 (1999). doi: 10.1038/8131; pmid: 10321251
33. Y. Zhao *et al*., The LIM-homeobox gene *Lhx8* is required for the development of many cholinergic neurons in the mouse forebrain. *Proc. Natl. Acad. Sci. U.S.A.* **100**, 9005–9010 (2003). doi: 10.1073/pnas.1537759100; pmid: 12855770
34. S. Nery, G. Fishell, J. G. Corbin, The caudal ganglionic eminence is a source of distinct cortical and subcortical cell populations. *Nat. Neurosci.* **5**, 1279–1287 (2002). doi: 10.1038/nn971; pmid: 12411960
35. O. Marín, S. A. Anderson, J. L. R. Rubenstein, Origin and molecular specification of striatal interneurons. *J. Neurosci.* **20**, 6063–6076 (2000). doi: 10.1523/JNEUROSCI.20-16-06063.2000; pmid: 10934256
36. S. Nóbrega-Pereira *et al*., Origin and molecular specification of globus pallidus neurons. *J. Neurosci.* **30**, 2824–2834 (2010). doi: 10.1523/JNEUROSCI.4023-09.2010; pmid: 20181580
37. X. Fan *et al*., Spatial transcriptomic survey of human embryonic cerebral cortex by single-cell RNA-seq analysis. *Cell Res.* **28**, 730–745 (2018). doi: 10.1038/s41422-018-0053-3; pmid: 29867213
38. G. Neves *et al*., The LIM homeodomain protein Lhx6 regulates maturation of interneurons and network excitability in the mammalian cortex. *Cereb. Cortex* **23**, 1811–1823 (2013). doi: 10.1093/cercor/bhs159; pmid: 22710612
39. Y. Zhao *et al*., Distinct molecular pathways for development of telencephalic interneuron subtypes revealed through analysis of Lhx6 mutants. *J. Comp. Neurol.* **510**, 79–99 (2008). doi: 10.1002/cne.21772; pmid: 18613121
40. E. Azim, D. Jabaudon, R. M. Fame, J. D. Macklis, SOX6 controls dorsal progenitor identity and interneuron diversity during neocortical development. *Nat. Neurosci.* **12**, 1238–1247 (2009). doi: 10.1038/nn.2387; pmid: 19657336
41. R. Batista-Brito *et al*., The cell-intrinsic requirement of *Sox6* for cortical interneuron development. *Neuron* **63**, 466–481 (2009). doi: 10.1016/j.neuron.2009.08.005; pmid: 19709629
42. N. Flames *et al*., Short- and long-range attraction of cortical GABAergic interneurons by neuregulin-1. *Neuron* **44**, 251–261 (2004). doi: 10.1016/j.neuron.2004.09.028; pmid: 15473965
43. M. C. Tiveron *et al*., Molecular interaction between projection neuron precursors and invading interneurons via stromal-derived factor 1 (CXCL12)/CXCR4 signaling in the cortical subventricular zone/intermediate zone. *J. Neurosci.* **26**, 13273–13278 (2006). doi: 10.1523/JNEUROSCI.4162-06.2006; pmid: 17182777
44. G. López-Bendito *et al*., Chemokine signaling controls intracortical migration and final distribution of GABAergic interneurons. *J. Neurosci.* **28**, 1613–1624 (2008). doi: 10.1523/JNEUROSCI.4651-07.2008; pmid: 18272682
45. G. Li *et al*., Regional distribution of cortical interneurons and development of inhibitory tone are regulated by Cxcl12/Cxcr4 signaling. *J. Neurosci.* **28**, 1085–1098 (2008). doi: 10.1523/JNEUROSCI.4602-07.2008; pmid: 18234887
46. J. A. Bagley, D. Reumann, S. Bian, J. Lévi-Strauss, J. A. Knoblich, Fused cerebral organoids model interactions between brain regions. *Nat. Methods* **14**, 743–751 (2017). doi: 10.1038/nmeth.4304; pmid: 28504681
47. L. Lim, D. Mi, A. Llorca, O. Marín, Development and functional diversification of cortical interneurons. *Neuron* **100**, 294–313 (2018). doi: 10.1016/j.neuron.2018.10.009; pmid: 30359598
48. C. Mayer *et al*., Developmental diversification of cortical inhibitory interneurons. *Nature* **555**, 457–462 (2018). doi: 10.1038/nature25999; pmid: 29513653
49. D. Mi *et al*., Early emergence of cortical interneuron diversity in the mouse embryo. *Science* **360**, 81–85 (2018). doi: 10.1126/science.aar6821; pmid: 29472441
50. F. J. Martini *et al*., Biased selection of leading process branches mediates chemotaxis during tangential neuronal migration. *Development* **136**, 41–50 (2009). doi: 10.1242/dev.025502; pmid: 19060332
51. M. Betizeau *et al*., Precursor diversity and complexity of lineage relationships in the outer subventricular zone of the primate. *Neuron* **80**, 442–457 (2013). doi: 10.1016/j.neuron.2013.09.032; pmid: 24139044
52. N. Kalebic, W. B. Huttner, Basal progenitor morphology and neocortex evolution. *Trends Neurosci.* **43**, 843–853 (2020). doi: 10.1016/j.tins.2020.07.009; pmid: 32828546
53. O. Marín, Cellular and molecular mechanisms controlling the migration of neocortical interneurons. *Eur. J. Neurosci.* **38**, 2019–2029 (2013). doi: 10.1111/ejn.12225; pmid: 23651101
54. A. Kepecs, G. Fishell, Interneuron cell types are fit to function. *Nature* **505**, 318–326 (2014). doi: 10.1038/nature12983; pmid: 24429630

55. R. Tremblay, S. Lee, B. Rudy, GABAergic interneurons in the neocortex: From cellular properties to circuits. *Neuron* **91**, 260–292 (2016). doi: 10.1016/j.neuron.2016.06.033; pmid: 27477017
56. B. Rudy, G. Fishell, S. Lee, J. Hjerling-Leffler, Three groups of interneurons account for nearly 100% of neocortical GABAergic neurons. *Dev. Neurobiol.* **71**, 45–61 (2011). doi: 10.1002/dneu.20853; pmid: 21154909
57. C. S. Raju *et al*., Secretagogin is expressed by developing neocortical GABAergic neurons in humans but not mice and increases neurite arbor size and complexity. *Cereb. Cortex* **28**, 1946–1958 (2018). doi: 10.1093/cercor/bhx101; pmid: 28449024
58. A. Alzu'bi, G. J. Clowry, Multiple origins of secretagogin expressing cortical GABAergic neuron precursors in the early human fetal telencephalon. *Front. Neuroanat.* **14**, 61 (2020). doi: 10.3389/fnana.2020.00061; pmid: 32982702
59. A. B. Muñoz-Manchado *et al*., Diversity of interneurons in the dorsal striatum revealed by single-cell RNA sequencing and PatchSeq. *Cell Rep.* **24**, 2179–2190.e7 (2018). doi: 10.1016/j.celrep.2018.07.053; pmid: 30134177
60. F. K. Wong *et al*., Pyramidal cell regulation of interneuron survival sculpts cortical networks. *Nature* **557**, 668–673 (2018). doi: 10.1038/s41586-018-0139-6; pmid: 29849154
61. O. Marín, Interneuron dysfunction in psychiatric disorders. *Nat. Rev. Neurosci.* **13**, 107–120 (2012). doi: 10.1038/nrn3155; pmid: 22251963
62. S. L. Wolock, R. Lopez, A. M. Klein, Scrublet: Computational identification of cell doublets in single-cell transcriptomic data. *Cell Syst.* **8**, 281–291.e9 (2019). doi: 10.1016/j.cels.2018.11.005; pmid: 30954476
63. L. Haghverdi, A. T. L. Lun, M. D. Morgan, J. C. Marioni, Batch effects in single-cell RNA-sequencing data are corrected by matching mutual nearest neighbors. *Nat. Biotechnol.* **36**, 421–427 (2018). doi: 10.1038/nbt.4091; pmid: 29608177
64. T. Stuart *et al*., Comprehensive integration of single-cell data. *Cell* **177**, 1888–1902.e21 (2019). doi: 10.1016/j.cell.2019.05.031; pmid: 31178118
65. A. Butler, P. Hoffman, P. Smibert, E. Papalexi, R. Satija, Integrating single-cell transcriptomic data across different conditions, technologies, and species. *Nat. Biotechnol.* **36**, 411–420 (2018). doi: 10.1038/nbt.4096; pmid: 29608179
66. C. Trapnell *et al*., The dynamics and regulators of cell fate decisions are revealed by pseudotemporal ordering of single cells. *Nat. Biotechnol.* **32**, 381–386 (2014). doi: 10.1038/nbt.2859; pmid: 24658644
67. X. Qiu *et al*., Reversed graph embedding resolves complex single-cell trajectories. *Nat. Methods* **14**, 979–982 (2017). doi: 10.1038/nmeth.4402; pmid: 28825705
68. J. Cao *et al*., The single-cell transcriptional landscape of mammalian organogenesis. *Nature* **566**, 496–502 (2019). doi: 10.1038/s41586-019-0969-x; pmid: 30787437


## ACKNOWLEDGMENTS

**Funding:** This work was supported by the National Key Research and Development Program of China (2019YFA0110101 and 2017YFA0103303 to X.W.; 2017YFA0102601 to Q.W.), the Strategic Priority Research Program of the Chinese Academy of Sciences (XDA16020601 and XDB32010100 to X.W.), the National Natural Science Foundation of China (NSFC) (81891001 and 31771140 to X.W.), the BUAA-CCMU Big Data and Precision Medicine Advanced Innovation Center Project (BHME-2019001 to X.W.), the Wellcome Trust (215556/Z/19/Z to O.M.), and Collaborative Research Fund of Chinese Institute for Brain Research (2020-NKX-PT-03). For the purpose of open access, the author has applied a CC BY public copyright license to any Author Accepted Manuscript version arising from this submission. **Author contributions:** X.W., O.M., and Q.W. conceived of the project and supervised research. T.L., B.W., and L.S. collected the samples. Y.S., Q.M., and Z.L. performed the scRNA-seq experiments. M.W., D.M., S.Z., and H.D. analyzed the scRNA-seq data. Y.S., Y.C., X.Z., and W.W. prepared the samples and carried out the immunofluorescent staining and image data analysis. J.Z. assisted with animal maintenance. Y.S., M.W., D.M., Q.W., O.M., and X.W. wrote the manuscript. All authors edited and proofed the manuscript. **Competing interests:** The authors declare no competing interests. **Data and materials availability:** The scRNA-seq data used in this study have been deposited in the Gene Expression Omnibus (GEO) under the accession number GSE135827. The supplementary materials contain additional data. All data needed to evaluate the conclusions in the paper are present in the paper or the supplementary materials.

## SUPPLEMENTARY MATERIALS

science.org/doi/10.1126/science.abj6641
Materials and Methods
Figs. S1 to S12
Tables S1 to S9
References (69–74)
MDAR Reproducibility Checklist
Movie S1

View/request a protocol for this paper from *Bio-protocol*.

25 May 2021; accepted 22 October 2021
10.1126/science.abj6641

Science

# Mouse and human share conserved transcriptional programs for interneuron development

Yingchao ShiMengdi WangDa MiTian LuBosong WangHao DongSuijuan ZhongYouqiao ChenLe SunXin ZhouQiang MaZeyuan LiuWei WangJunjing ZhangQian WuOscar MarínXiaoqun Wang

*Science*, 374 (6573), eabj6641. • DOI: 10.1126/science.abj6641

**Surveying brain interneuron development**

As transient structures in early brain development, the ganglionic eminences generate dozens of different types of interneurons that go on to migrate throughout and weave together the developing brain. Shi *et al*. analyzed human fetal ganglionic eminences. Single-cell transcriptomics revealed unexpected diversity in the types of progenitor cells involved. The human ganglionic eminence depends more heavily on intermediate progenitor cells as workhorses than does the developing neocortex, with its greater reliance on radial glial cells. —PJH







*Science* (ISSN ) is published by the American Association for the Advancement of Science. 1200 New York Avenue NW, Washington, DC 20005. The title *Science* is a registered trademark of AAAS.